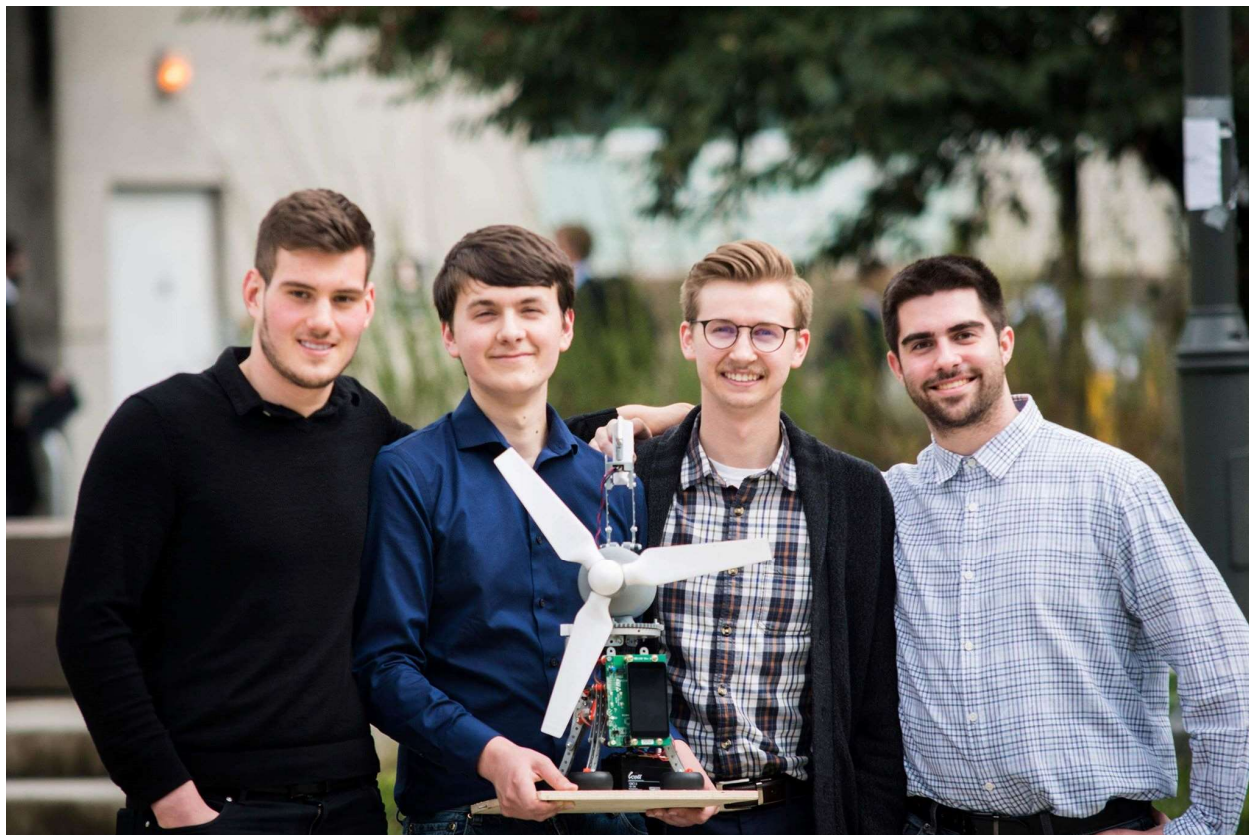


Wind Turbine Project Report



Member	Student Number
Grant Andersen	36881167
Marko Markusi	58041930
Igor Vuckovic	40107161
Jared West	72807043

Table of Contents

Project Overview	8
Summary	8
Requirements	8
Constraints	9
Goals	9
Task 1: Generator.....	10
Requirements	10
Constraints	10
Goals	10
Design	10
Validation.....	11
Rotor	11
Stator	12
Case.....	14
Task 2: Boost Converter	15
Requirements	15
Goals	15
Constraints	15
Power Rectifier Design	16
Power Rectifier Validation	17
Boost Converter Design.....	17
Boost Converter Validation	20
Final Circuitry Values.....	22
Task 3: Controller	23
Requirements	23
Goals	23
Constraints	23
Design	24
ADC	25
DMA	27
Stepper Motor	28
Boost Converter	29
LCD.....	29

Maximum Power Point Tracking.....	30
Validation.....	31
ADC	31
Stepper Motor	31
LCD.....	31
Maximum Power Point Tracking.....	31
Task 4: Sensing and Modeling.....	32
Voltmeter	32
Requirements and Goals	32
Design	32
Validation.....	33
Ammeter	34
Requirements and Goals	34
Design	34
Validation.....	35
Wind Direction Sensor.....	35
Requirements and Goals	35
Design	35
Validation.....	36
Stepper Motor Controller.....	36
Design	36
Validation.....	37
Output Voltage Controller	37
Design	37
Validation.....	38
Perturb and Observe Algorithm	39
Design	39
Integration Process.....	40
Power Electronics with Generator	40
Sensors with Power Electronics and Controller.....	41
Stepper Motor Control and Maximum Power Point Tracking Testing.....	41
Battery Charging and Powering Connections.....	41
Final Construction and Testing with Fans	42

References.....	43
Appendix.....	45
Timeline:	45
Budget:	46

Table of Figures

Figure 1.1: Magnet Pole Orientation.....	11
Figure 1.2: 4-Pole 16 Magnet Configuration	11
Figure 1.3: 8-Pole 16 Magnet Configuration	11
Figure 1.4: Iron Stator Ring.....	13
Figure 1.5: Winding Configuration.....	14
Figure 1.6: Generator Assembly-Ready for Integration	14
Figure 2.1: Three Phase Diode Rectifier Prototype	16
Figure 2.2: 1N5819 (left) and SB530 (right)	16
Figure 2.3: 100 μ F 220 μ F and 1000 μ F Filtering Capacitor Simulations	17
Figure 2.4: Second Iteration Boost Converter	18
Figure 2.5: Third Iteration PCB Design and Completed Circuit	19
Figure 2.6: Final Iteration of the Power Electronics Circuitry.....	20
Figure 2.7: PCB Layout of the Final Iteration	20
Figure 2.8: Third Iteration (left) and Final Iteration (right).....	21
Figure 2.9: Testing Microcontroller PWM with Boost Converter.....	21
Figure 3.1: STM32F769I DISCOVERY Board.....	24
Figure 3.2: CubeMX Software.....	25
Figure 3.3: ADC Hardware Model	26
Figure 3.4: ADC Using DMA.....	27
Figure 3.5: ADC Buffer Array Contents.....	27
Figure 3.6: 5V Unipolar Stepper Motor.....	28
Figure 3.7: Half-Step Drive Pulse Sequence	28
Figure 3.8: Half-Step Drive Coil Excitation	28
Figure 3.9: Boost Converter Circuit with Switching MOSFET.....	29
Figure 3.10: LCD Panel Displaying Readings.....	29

Figure 3.11: Boost Converter Control Algorithm	30
Figure 4.1: Voltmeter Circuit.....	32
Figure 4.2: Voltmeter CircuitMaker Plot.....	33
Figure 4.3: Plot of Voltmeter Gain vs Voltage Signal to Microcontroller.....	33
Figure 4.4: Ammeter Circuit.....	34
Figure 4.5: Ammeter CircuitMaker Plot.....	35
Figure 4.6: Plor of Ammeter Gain vs Voltage Signal to Microcontroller.....	35
Figure 4.7: Fin on Wind Vane	35
Figure 4.8: Stepper Motor Control Loop	36
Figure 4.9: Stepper Motor Simulation Output	37
Figure 4.10: Output Voltage Control Loop.....	37
Figure 4.11 Boost Converter Bode Plot.....	38
Figure 4.12: Voltmeter Bode Plot.....	38
Figure 4.13: Output Voltage Simulation Output.....	38
Figure 5.1: Power vs Resistance Curve	40
Figure 5.2: Battery Charging Circuit Conection Diagram.....	42
Figure 5.3: Final Product	42

Table of Acronyms

ADC	Analog-to-Digital Converter
AWG	American Wire Gauge
BSP	Board Support Package
CCM	Continuous Conduction Mode
DCM	Discontinuous Conduction Mode
DMA	Direct Memory Access
LSB	Least Significant Bit
MMPT	Maximum Power Point Tracking
RTOS	Real-Time Operating System
STM	STMicroelectronics
TFT	Thin-Film-Transistor
VDDA	Analog Voltage Supply

Project Overview

Summary

The project is a fully functional prototype of a wind turbine. The project tasks are divided among four electrical engineering students and include making a generator, converting the raw power into usable power, sensing multiple inputs, modelling different components to the system, and programming a controller.

Of the previously mentioned tasks, Igor Vuckovic is in charge of the generator, Jared West is in charge of the power conversion, Grant Andersen is in charge of sensing and modeling the system, and Marko Markusi is in charge of the controller's programming.

All wind turbines have several components in common - a generator, power electronics, sensors, and a controller. For a company to stand out in industry, its designs will need to have certain unique aspects and must be economically viable. These aspects including having a touch screen capable of receiving commands and displaying output power and using a battery charging circuit to both charge a battery and use the battery's power for the microcontroller's use.

Requirements

The following aspects of the overall design are required for proper functionality of the wind turbine prototype:

- Have a PMSG outputting multiple phases of voltages to the rectifier
- Have a rectifier with several phases to match the generator
- Have a boost converter capable of increasing and decreasing current being drawn by PWM control
- Have sensors able to read output voltage and current, and by extension of that output power
- Use a wind direction sensor able to map voltages to positions
- Have a microcontroller capable of outputting both a PWM signal and being able to read ADC values from the sensors
- Have a brake ability to safely and securely stop turbine blades in dangerous conditions
- Have a motor to properly control the direction the wind turbine is facing

Constraints

Throughout the project, we will be facing various challenges due to the nature of our work. In particular, we cannot use many off-the-shelf components. For instance, we will not be using any single board computers, rather we will be using a programmable microcontroller. In addition, we will need to restrict our design to fit within a space of 50 cm in width by 50 cm and in length by 60 cm in height. The project is also limited to a budget of \$1000 for creation of the final prototype where any money spent over \$500 deducts points from the maximum achievable grade for this course.

Goals

The project's primary goal is to create a sustainable and robust system that can meet a variety of different energy demands. This goal can be divided into several, more specific goals:

- Generate and regulate output voltage between 10V and 15V
- Generate at least 1.3 watts of power to accommodate a variety of different loads
- Create a self-sufficient system that charges its own battery for operation during low or no wind situations
- Full 360-degree rotation and 300-degree wind detection to accommodate for changes in wind direction
- Have an easy-to-use user interface
- Be able to override software control of the motor in dangerous situations

Task 1: Generator

The generator is the most vital component of any wind turbine system as it converts mechanical power into electrical power which, upon being rectified and regulated, is then be utilized at the load. As a result, all requirements must be met for the generator to function and for it to work with all other components of the wind turbine system.

Requirements

- Must be a permanent magnet synchronous generator
- Must produce at least 6 volts and 200 milliamps DC (1.2 watts) after the rectifier

Constraints

- The rotating blades of the turbine are to be attached to the rotor of the generator and must fit within the following dimensions: 50 cm in length, 50 cm in width, and 60cm in height

Goals

- Operate at an average 1000 RPM
- Produce minimal cogging such that the blades can start up without assistance
- Minimize winding resistance to reduce losses
- Produce at least 2 watts of power
- Operate at higher voltage and lower current to minimize losses

Design

- External stator and internal rotor
- 8 pole internal rotor with 16 neodymium magnets
- 6 slot external stator with 150 turns per winding (26 AWG magnet wire)
- 3 phase system with 300 turns per phase
- Phase resistance of $4.2\ \Omega$
- 2 mm gap between rotor and stator (1mm plastic, 1mm air)

Validation

Rotor

To maximize the flux, compact magnets with a high flux density were required and as a result the 8110 rectangular magnets from Radial Magnet Inc. were chosen. These magnets were ideal for the rotor as the magnetic poles were oriented such that the flux flowed out of the narrow ends of the magnet as shown in the figure below.

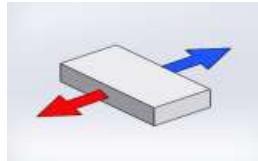


Figure 1.1: Magnet Pole Orientation

Before the iron core was implemented, several iterations of the rotor were tested. Different amounts of magnets and different orientations were tested with a 6 slot, 3 phase, 300 turn per phase stator with 30 AWG magnetic wire and a drill operating at 600 RPM. Using 16 magnets produced better results than with 8 magnets as expected and the waveforms were very similar which meant that potential cogging problems in the future could be addressed by decreasing the number of magnets while maintaining the same number of poles. Three tests were conducted with 16 magnets: 4 poles, 8 poles, and 16 poles. Although the 16-pole design produced a waveform that most accurately resembled a sinusoid, the voltage observed was significantly lower than the 4 and 8 pole tests. Below are the results of the 4-pole (left) and 8-pole (right) tests. The 8 pole 16 magnet configuration was chosen as it produced a clean waveform with the highest peak to peak voltage.

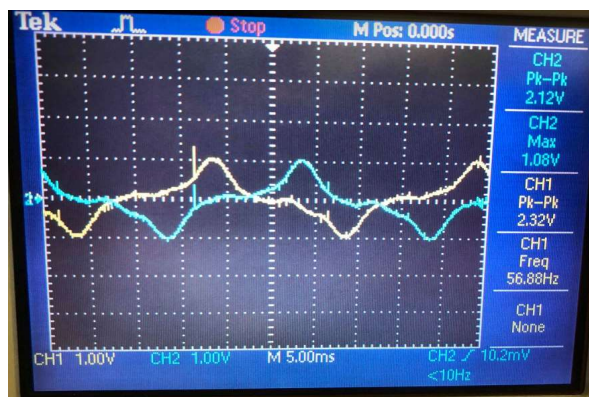


Figure 1.2: 4-Pole 16 Magnet Configuration

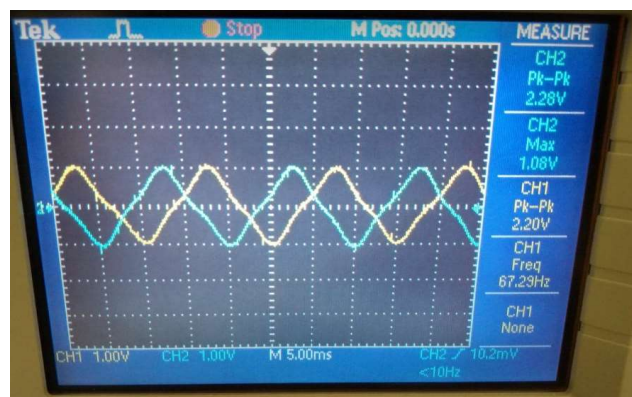


Figure 1.3: 8-Pole 16 Magnet Configuration

Upon waterjet cutting the stator, the air gap between the rotor and the stator had to be optimized. Three different gaps: 3 mm, 2 mm, and 1.5 mm, were tested with 3D printed rotors, each housing 16 magnets in an 8-pole configuration. Each of the gaps includes 0.5mm of plastic which prevented the magnets from detaching from the rotor. With the blades mounted to the shaft each of the rotors was tested with the fan. With a 3 mm gap the blades started spinning immediately after the fan was switched on and reached maximum speed relatively quickly. With the 2 mm gap the blades took longer to start up and reach top speed and with the 1.5 mm gap the blades couldn't overcome the cogging and start spinning on their own. As a result, the 2 mm gap was selected as it maximized the flux while also allowing the blades to start up on their own.

Relative to the reluctance of the gap, the reluctance of a plastic rotor does not have a huge impact on the magnetic circuit and replacing it with an iron one would not lead to a significant improvement. Although there would be an improvement in the overall flux density of the rotor, there would also be an increase in the amount of cogging as well. Should the increased cogging have been too much for the blades to start up on their own, the amount of time and money required to adjust the gap would have been too high considering the marginal gain that the waterjet cut rotor would provide.

Stator

In a study, Performance Comparison of Internal and External Rotor Structured Wind Generators Mounted from Same Permanent Magnets on Same Geometry, conducted by İ. Tarımer and C. Ocak it was determined that an external stator machine produced more power at higher RPM than an internal stator machine. Although an internal stator machine has lower copper weight and armature steel weight due to a compact design, it also has high armature thermal load, copper loss and current density which makes it less efficient than an external rotor machine. Based on this study and the resources available, an external stator design was chosen.

A 3-phase system was chosen because it provided a higher average power when compared to 1 and 2 phase systems. A 3-phase system also produces a much steadier DC signal after being rectified as increasing the number of phases decreases ripple voltage.

Using the following equation, the required number of turns was determined for a target peak voltage at a specific RPM.

$$V_{peak} = \sqrt{2} * 4.44 * \frac{RPM * \#poles}{120} * Flux * \# of turns$$

According to the datasheet for the 8110 magnets, the flux density of the magnets is 0.48 T and the dimensions of the cross-sectional area are 25.4 mm by 3.175 mm. For a target peak voltage of 5 V at the average speed of the blades across all 3 fan speeds, which we found to be approximately 1000 RPM, 308 turns (approximately 300) per phase were required. Due to the physical size constraints of the iron core, 26 AWG wire had to be used instead of 24 AWG and 150 turns were wound on each slot of the stator in order to achieve the desired 300 turns per phase. Upon testing the design with 300 turns per phase, we observed a peak voltage of up to 9.3 V which was double the calculated value. This is likely a result of the way the flux was calculated as the iron core was not considered in the formula. The almost twofold increase in voltage resulted in an average 12 Volts DC after being rectified which in turn minimized the losses as the boost converter could be operated on a much lower duty cycle.

In earlier prototypes, a bobbin design was used to allow for easy winding, but the design was impractical to waterjet cut and so the design was changed to use rings like the one in figure 1.4.

The main challenge with this design was that applying the magnetic wire directly onto the iron core caused it to short through the iron regardless of the powder coat on the iron and the insulation of the wire. To solve this problem, the inside iron stator was coated in electrical tape to act as further insulation.

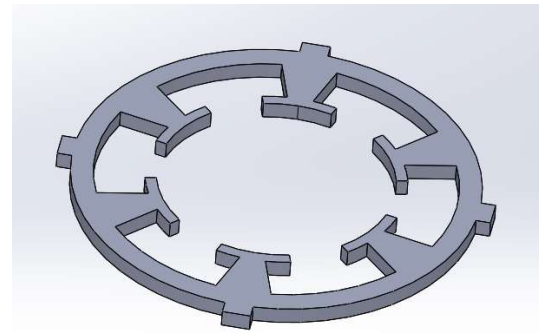


Figure 1.4: Iron Stator Ring

The connections between each of the windings was done according to an online winding calculator for a wye configuration. Figure 1.5 below illustrates the connections made.

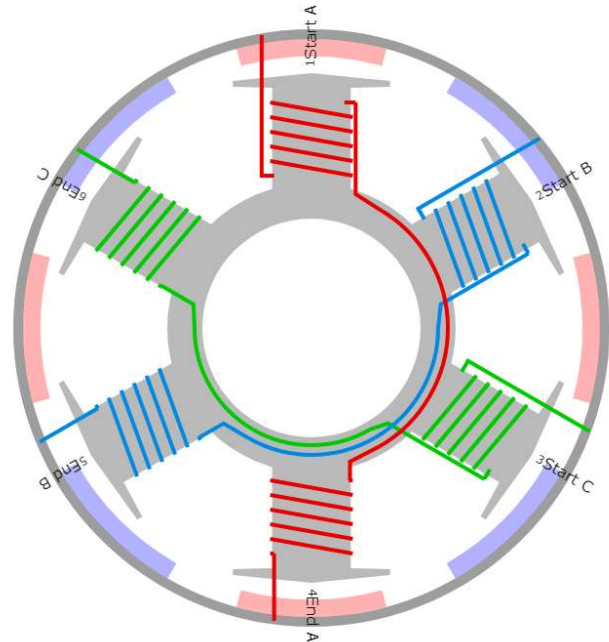


Figure 1.5: Winding Configuration

Case

A case was designed to hold in place the stator rings and to hold the rotor in place with a set of ball bearings. To ensure that the axle, which holds both the blades and the rotor, was perfectly concentric with the stator, the lid and bottom piece were designed with a lip so that the parts would fit together and be unable to move. The case was designed with the integration phase in mind as it left a flat face with mounting holes where a backpiece that would contain the PCB could be attached. Likewise, two slots were cut out along one of the mounting screws such that the generator itself could be attached to another piece. Figure 1.6 below shows the stator case and Figure 1.7 shows the final generator assembly with components ready for integration.

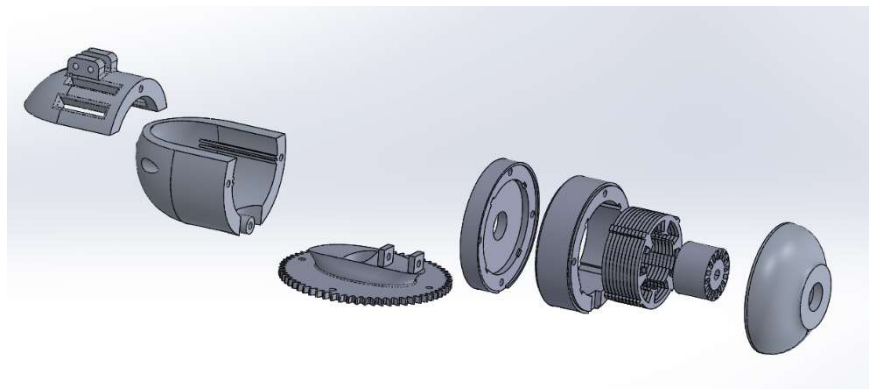


Figure 1.6: Generator Assembly Ready for Integration

Task 2: Boost Converter

Power electronics are used to control the electrical power within a system. The wind turbine utilizes this area of study to optimize the power being produced by the generator. The system takes random AC power being produced by the spinning of the generator and converts it into usable DC power with the help of a fine-tuned controller and various sensors. The required power electronics for this project are a n-phase rectifier and a boost converter.

Requirements

- Must take AC voltage waveforms, from the generator, and convert them into 12V DC (10V-15V).
- The completed power electronic circuit is designed and fabricated on a PCB in an organized and compact design with proper power trace routing.

Goals

- Minimize losses due to the equivalent resistive components. The reduction of the equivalent series resistance allows for most of the power to be consumed by the load – maximizing the power of the circuit.
- Maintain a power efficiency of 90% and greater

Constraints

- The rectifier converts n-phases which depends on the generator into a DC voltage.
- The boost converter circuit requires a PWM signal to operate the MOSFET. The controller, which supplies the PWM signal, emits a 3.3V logic signal max. For the circuit to work, the MOSFET must be able to operate at 3.3V.
- For design purposes, the PCB must fit exactly within the turbine compartment at the top. To maintain the overall aerodynamic shape and the neatness of the finished structure.

Power Rectifier Design

The rectifier, comprised of six diodes and a filtering capacitor, is designed by simulations using the circuit simulator Multisim. The six diodes are chosen due to the number of phases supplied by the generator. A 220 μF filtering capacitor is added in parallel to the diode bridge to filter out any of the residual AC voltages. The value of the capacitor is determined through simulation. Due to the budget constraints, the diodes are chosen based on simulations as well. Initially, the 1N5918 diodes were used for the first tests along with the first demo – seen in figure 2.1 [3].

These diodes have a low forward voltage drop of 600mV at 1A average rectified current. The 1N5819 Schottky diodes were compared with the SB530 Schottky diodes using the simulator which justified the decision to move forward with the SB530 diodes – shown in the figure below [4].

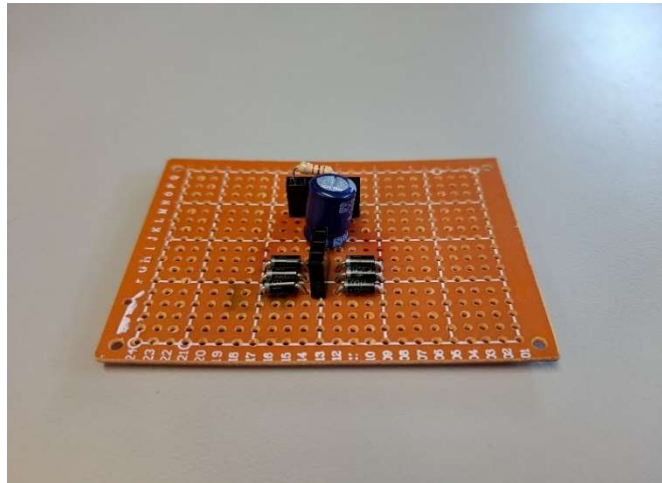


Figure 2.1: Three Phase Diode Rectifier Prototype

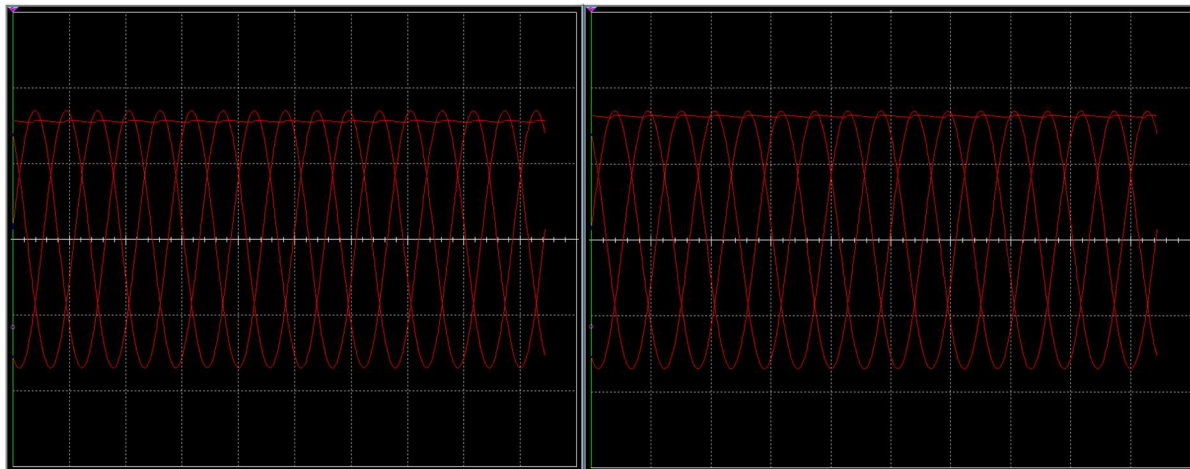


Figure 2.2: 1N5819 (left) and SB530 (right)

The SB530 diodes show a greater rectified voltage given the same input three-phase voltage – no filtering capacitor.

Power Rectifier Validation

The voltage out of the rectifier is bumpy. The electrical engineering equivalent of a clothing iron is used to produce the smooth DC voltage – a capacitor. Although any capacitor would have filtering properties, simulations are used to determine the optimal capacitance value – saving space and money.

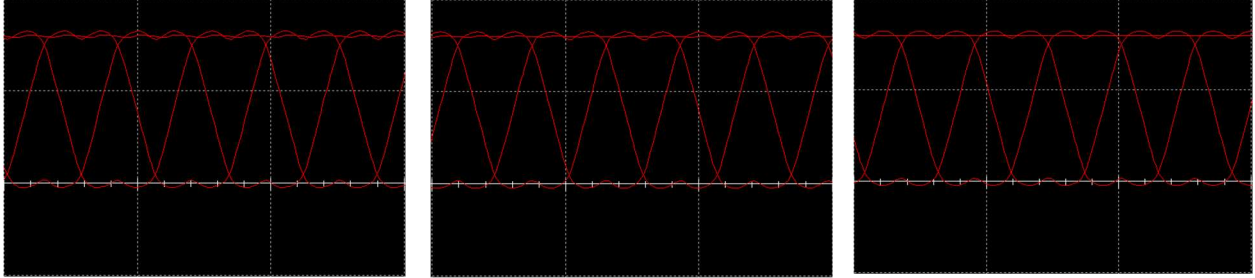


Figure 2.3: 100µF 220µF and 1000µF Filtering Capacitor Simulations

The 1000 µF produces complete DC voltage signal out of the simulated rectifier, however, the 220µF capacitor provides an equally flat signal. The 220 µF filtering capacitor is used for the duration of the project – rated at 35V for safety measures.

Boost Converter Design

The first prototype of the boost converter was initially built on a breadboard with uncalibrated components. This first circuit had boost characteristics, however, after consulting with a teaching assistant it was determined that the circuit was operating in DCM. After following a video which was produced by UBC that covers the necessary components and equations, a proper boost converter that operates in CCM was designed [5].

For the calculations, the inductor was set at a constant value. There are six values the equations give to create a working circuit: duty cycle, D ; current through the inductor, I_L ; current ripple, Δi_L ; switching frequency, f_{sw} ; voltage ripple, Δv_c ; and the output capacitance needed, C_v . Their equations are as follows:

$$\begin{aligned} \frac{V_{out}}{V_{in}} &= \frac{1}{1-D} \rightarrow D = 1 - \frac{V_{in}}{V_{out}}, & I_L &= \frac{V_{out} I_{out}}{V_{in}} = \frac{V_{out}^2}{R_{Load} V_{in}}, & \Delta i_L &= \%_{current\ ripple} * I_L, \\ f_{sw} &= \frac{V_{in} D}{L \Delta i_L}, & \Delta v_c &= \%_{voltage\ ripple} * V_{out}, & C &= \frac{V_{in} D}{f_{sw} (1-D) R_{Load} \Delta v_c} \end{aligned}$$

Designing a 1:2 boost ratio, there are constant values for the calculations. $V_{in} = 6V$, $V_{out} = 12V$, $R_{load} = 100\Omega$, $L = 1.111mH$, current ripple = 20%, voltage ripple = $\pm 2\%$. The calculations give a duty cycle of 50%, $I_L = 0.24A$, $\Delta i_L = 0.048A$, switching frequency = 56.2kHz, $\Delta V_C = 0.48V$, $C = 2.22\mu F$. Putting the selected components together on the bread board creates a properly working converter.

Using a multimeter to determine the voltage and current values, for the input and output, the respective power values are calculated. The efficiency of the circuit designed is 93% which is within the goal of the power electronics. The circuitry does not need drastic changes, but further testing is done to create a more efficient system.

The second iteration of the converter design involves determining the areas where losses can be reduced and soldering the circuit onto a perforated board. The same 1.111mH inductor and the IRFZ44N MOSFET were used in this design of the converter [6]. The inductor and MOSFET have a resistance of 0.52Ω and

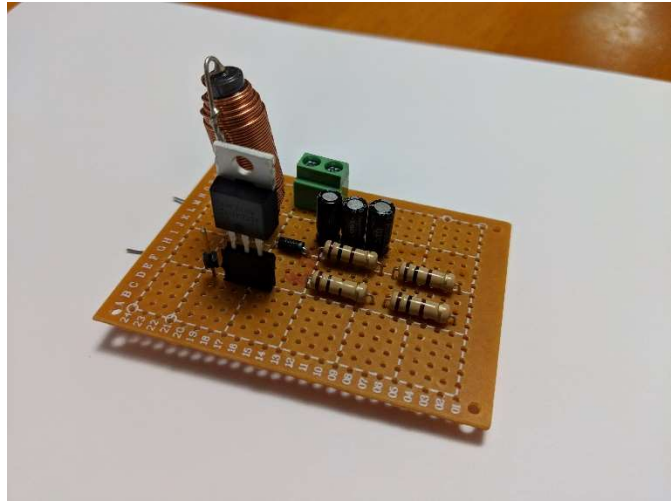


Figure 2.4: Second Iteration Boost Converter

$17.5m\Omega$ respectively. To reduce the equivalent series resistance of the capacitor, three electrolytic capacitors are soldered in parallel – reducing the overall resistance. The circuit is placed on the perforated board to reduce the parasitic capacitance that the breadboard introduces. The inductor is rated for 1A [7].

Iteration three of the boost convert design revolves around transferring the completed circuit onto a printed circuit board for neatness and to reduce any human error in soldering traces. The same inductor and MOSFET from the second iteration are used for the third.

Changes from the second iteration:

- Using a single 100 Ω 10W power resistor [8]
- Using a larger 220 μ F electrolytic capacitor in parallel with a 1.5nF foil capacitor
- Designing and soldering circuit onto PCB

The circuit is constructed and tested to verify the components are operating as intended. The third iteration also requires for a small test to determine whether the microcontroller can operate the MOSFET within the boost converter circuit. The PCB design, along with the completed PCB can be seen below.

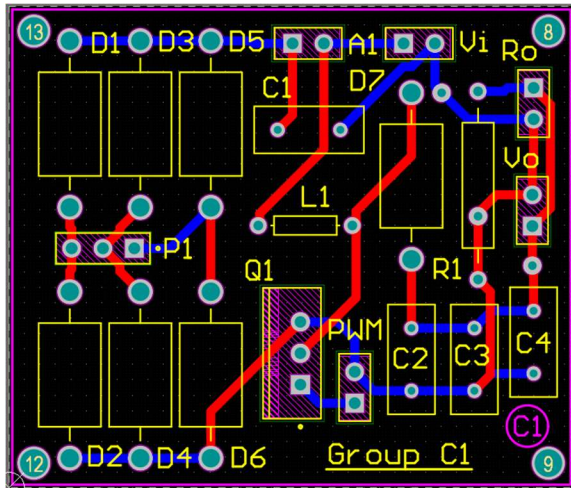


Figure 2.5: Third Iteration PCB Design and Completed Circuit

The circuit constructed for the third iteration is to demonstrate the working circuit. The circuit also produces an efficiency of 95%.

The final iteration required the integration of sensors along with dimensional altering to accommodate the final product.

Changes from the third iteration:

- Upgrading to a 1.012mH toroidal inductor with 0.135 Ω resistance [9]
- Upgrading to the IRLB8721 MOSFET [10]
- Integration of a voltmeter and ammeter

- Widening the circuit to 73 mm for the turbine case
- Upgrading the connectors to power electronics grade terminal blocks [11]

With this iteration, final testing is completed to verify the circuitry works as it should. The final board also requires the testing with the sensing & modeling and with the microcontroller group members.

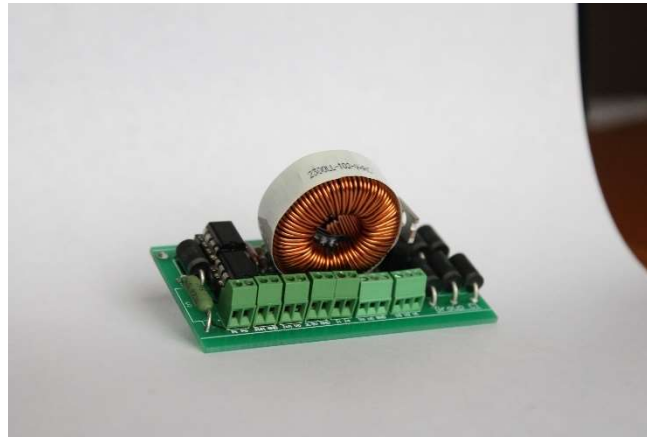


Figure 2.6: Final Iteration of the Power Electronics Circuitry

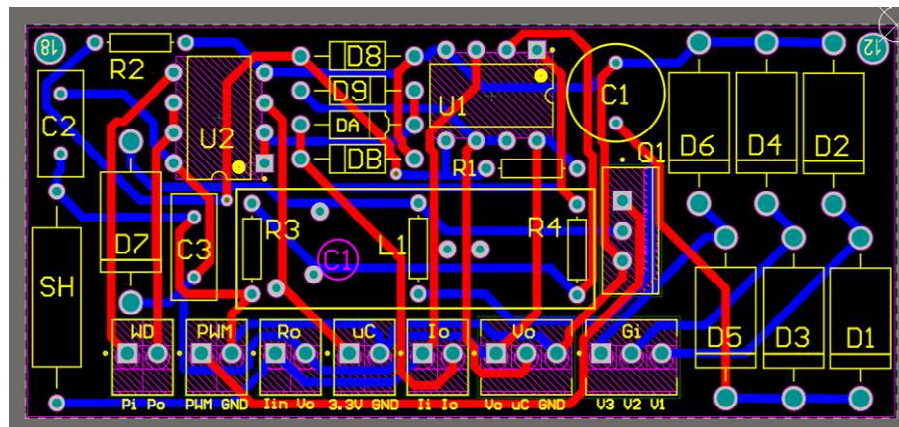


Figure 2.7: PCB Layout of the Final Iteration

Boost Converter Validation

Each iteration improved upon the design, by accommodating the constraints put upon the task and completing the goals! For the final design, each component was selected with simulation and testing. The inductor was upgraded to reduce the overall resistance seen in the circuit to allow for the maximum current and voltage to be seen at the output. Justification was done by simulating the circuits with the inductor equivalent resistance, seen in the figure below.

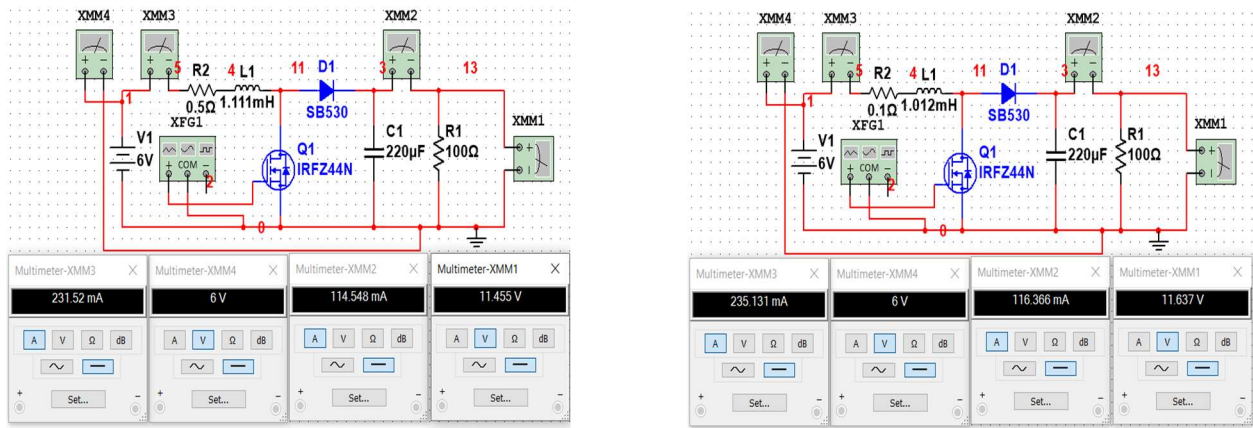


Figure 2.8: Third Iteration (left) and Final Iteration (right)

The output voltage produced is 200mV higher with the upgraded inductor, creating more of an ideal 1:2 boost converter – due to the lower resistance seen by the circuit.

The MOSFET is tested with the circuit to determine whether a gate driver is required to drive the switch of the circuit. The microcontroller is programmed to produce a PWM signal at 56.2kHz with a duty cycle of 50% and then connected to the boost converter circuit – seen in figure 2.9.

Testing with the microcontroller demonstrated a working boost converter circuit without the need for the gate driver – simplifying the final circuit design.

The diode used was simulated with the rectifier. The low voltage drops of the diode with the supplied current justified the use of the SB530 Schottky diode. To maintain the efficiency, a low voltage drop is sought out for.

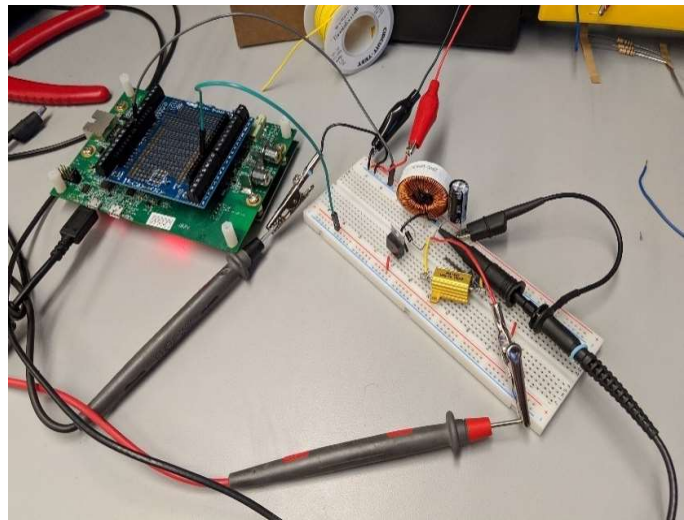


Figure 2.9: Testing Microcontroller PWM with Boost Converter

The capacitor is tested with the completed circuit. The calculated minimum capacitor value is 2.2μF with a voltage ripple of $\pm 2\%$. This ripple was reduced by increasing the value of the capacitor to 220μF

which created a voltage ripple of $\pm 0.02\%$. A low ripple produces flat DC voltage out of the converter; however, the higher capacitance will require more time to charge in this circuit.

The load resistor of 100Ω was determined to be the optimal load from testing with the generator. A series of tests were completed with different loads, recording the different values of voltage and current. With lower loads, the turbine could not get up to speed as quickly but produced more current. Alternatively, higher loads provided with the complete opposite. The 100Ω resistor provided with a quick turbine spin up with enough current to produce 2-3 watts of power.

Final Circuitry Values

From the designing of the circuitry to the validation, optimal component values were determined and implemented into the final PCB. While changing the various component values, the boost converter equations were used to maintain a properly working circuit. For the final implementation, the circuit values are as follows:

- 7 x SB530 Schottky Diodes (6 for rectifier, 1 for converter)
- 1.111mH Toroidal inductor
- IRLB8721 MOSFET
- 2 x 220 μ F electrolytic capacitor (filtering and boost)
- 1.5nF foil capacitor
- 100Ω 10W power resistor
- 62kHz switching frequency

The power electronic circuit is vital for the creation of a fully self-sufficient wind turbine. The trace widths on the PCB are 0.8mm in thickness to accommodate for a maximum current of 2 amps. The trace widths also increased to reduce the resistance of the traces to help reduce power losses through the circuit.

Task 3: Controller

The purpose of the microcontroller is to control the overall operation of the wind turbine. The controller uses readings from the wind direction sensor to keep the generator aligned with the wind to maximize power generation. Through voltage and current readings from the load, the controller also changes the duty cycle of the boost converter to maximize power and control the speed of the blades.

Requirements

- Read values from current and voltage sensors at the load to calculate the generated power
- Use an MPPT algorithm based on the current and previous power calculations, the controller changes the duty cycle of the PWM applied to the boost converter's switching MOSFET to maximize power generation
- Drive a stepper motor to align the wind turbine with the wind direction
- Display the voltage, current and power readings to the user.

Goals

- Display relevant information on an LCD screen directly connected to the microcontroller instead of the transmitting the data to another device to create an independent system
- Receive touch input from the user allowing manual control of the wind turbine's functions.

Constraints

- The hardware platform used for the controller must use a microcontroller and cannot use a single-board computer.
- The control implements a closed-loop wind-tracking system and MPPT algorithm to control blade speed and power.
- Controller code must be non-blocking and interrupt driven to ensure sensor readings are taken asynchronously and acted upon regularly and in a timely manner.

Design

The design for the controller was centered around STMicroelectronic's 32F769I DISCOVERY kit (Figure 3.1), which features a STM32F7 series microcontroller based on the ARM®Cortex®-M7 core.

The controller is equipped with the following key features:

- ARM®Cortex®-M7 core with a 216MHz clock speed
- 2 Mbytes of Flash memory and 512+16+4 Kbytes of RAM
- On-board ST-LINK/V2 in-circuit debugger and programmer
- Chrom-ART graphical hardware accelerator
- LCD-TFT controller
- 4" capacitive touch LCD display
- 512-Mbit Quad-SPI Flash memory
- 128-Mbit SDRAM
- 10 16-bit timers
- 2 32-bit timers
- 3 12-bit ADCs (24 channels)
- 16-stream DMA controller with FIFOs and burst support
- 4 I2C interfaces
- Up to 168 I/O ports with interrupt capability
- Arduino™ Uno V3 connectors for use with Arduino based shields



Figure 3.1: STM32F769I DISCOVERY Board

An STM32 development board is used instead of an Arduino based board because it allows for greater control of the I/O and peripherals as Arduino boards tend to abstract the hardware which does not allow for proper utilization of the hardware's performance. Using the STM32 allows for scalability if the wind turbine prototype was to be developed into an actual product. An Arduino would not have the performance necessary for a full-scale product and would rely on maintenance of public written libraries.

While ARM based microcontrollers feature high performance and low power consumption, the configuration of I/O and peripherals can be quite daunting and involves multiple steps to toggle an output pin. To reduce development time STMicroelectronics' STM32CubeMX (Figure 3.2) initialization code generator software was used to set up various I/O and peripherals. The tool provides a graphical interface for configuring peripherals and generates the necessary code needed to configure the peripherals. The code generated by the CubeMX software (Figure 3.2) uses comments to parse where the user is supposed to insert their own code, so it is not overwritten if a peripheral configuration changes and the code is regenerated. The structure of the template generated by the program adds un-necessary bloat to the project and makes the code hard to read. Therefore, after all the I/O and peripherals were defined for the project and fully configured, the configuration code was transferred to a simpler and cleaner template improving the readability of the project.

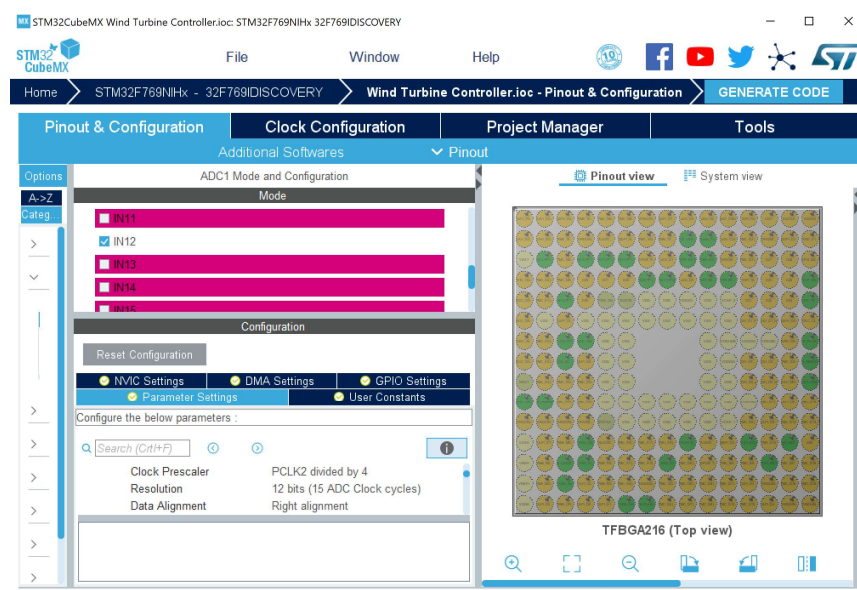


Figure 3.2: CubeMX Software

ADC

The controller uses three external ADC channels to measure and calculate:

- Voltage at the load
- Current at the load
- Wind direction position

The ADC used inside the STM32F769NI is a successive approximation analog-to-digital converter. It performs a conversion by quantizing the continuous signal into a discrete signal using a binary search algorithm. A high-level model of the hardware used in the ADC can be found in the ADC application note provided by STM [14] (Figure 3.3).

The fastest rate at which the signal can be sampled depends on the maximum frequency of the

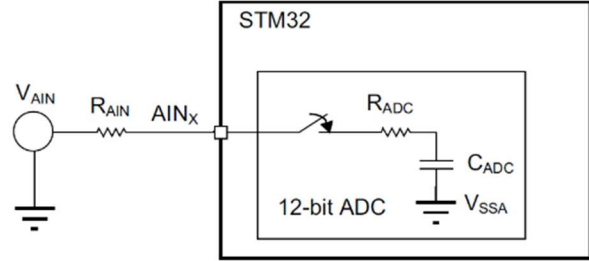


Figure 3.3: ADC Hardware Model

signal and per the Nyquist-Shannon sampling theorem the sampling

frequency should be at least twice the maximum frequency of the signal. Due to the sampling capacitor used in the ADC the RC time constant (τ) of the ADC depends heavily on the impedance of the source signal. To ensure that the sampled data is valid, the minimum sampling rate, which depends on the input impedance (R_{AIN}) seen by the ADC, must be calculated. For this reason, all the ADC signals are passed through a buffer op-amp to reduce the input impedance seen. The datasheet [15] provides a formula for calculating the minimum sampling rate (k):

$$R_{AIN} = \frac{(k - 0.5)}{f_{ADC} * C_{ADC} * \ln(2^{N+2})} - R_{ADC}$$

Using the typical values of C_{ADC} and R_{ADC} from the datasheet with a 25MHz ADC:

- Taking R_{AIN} to be approximately 10 Ω (ADC signals are feed through an LM358N buffer amplifier)
- We find the minimum value of k to be 7 for the external ADC channels

The 12-bit ADC works by mapping voltage readings from 0 to 4095, where 0 corresponds to 0V or GND and 4095 corresponds to the analog supply voltage (VDDA). The nominal value for VDDA is typically assumed to be 3.3V, but the analog supply voltage depends on the internal voltage reference, regulation of the power supply and temperature. To get the most out of the ADC, STM's ADC application note [14] recommends calculating the value of VDDA instead of using the nominal value. To ensure

voltages are correctly mapped to ADC values the internal voltage reference can be sampled and measured using one of the internal ADC channels, from there the current value of VDDA can be calculated.

To accurately sample the internal voltage reference (V_{REFINT}) data, the datasheet [16] specifies a minimum sampling time ($T_{S_vrefint}$) of 10 μ s. With an ADC running at 25MHz the minimum sampling rate is calculated to be: 25 clock cycles. Choosing the next closest sample rating for the external and internal ADC channels a sampling rate (k) of 28 is used.

Meeting the minimum sampling rate requirements of the ADC channels guarantees an accuracy with maximum error of $\frac{1}{4}$ LSB with a 12-bit ADC and 3.3V analog supply:

- $1 \text{ bit} = \frac{3.3V}{2^{12} \text{ bits}} = 0.80466mV$
- $Accuracy = \frac{1}{4} \text{ LSB} = \frac{0.80566mV}{4} = 0.201416mV$

DMA

The ADC is used alongside a DMA controller to transfer the sampled data without the usage of the CPU. The ADC is triggered every 100ms by a timer interrupt, the channels are sampled, and the data is then transferred to a buffer array in RAM by the DMA (Figure 3.4). Each channel is sampled 16 times (Figure 3.5) before the ADC conversion sequence is

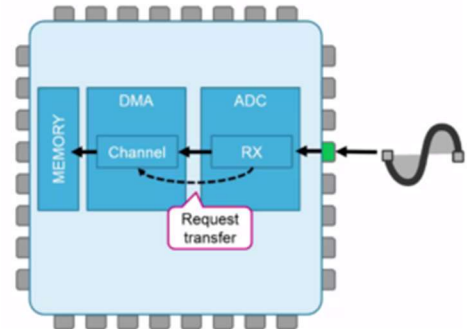


Figure 3.4: ADC Using DMA

completed. The samples are then filtered using an oversampling filter before being used. While averaging the readings does not necessarily improve accuracy, it negates the effect of ripple seen in the voltage and current readings.



Figure 3.5: ADC Buffer Array Contents

Stepper Motor

A 5V unipolar stepper motor (Figure 3.6) is used to rotate the top assembly of the wind turbine. To deliver enough current to excite the stepper motors coils, a driver board, which includes a ULN2003 transistor array, is used. To increase step precision, the stepper motor is driven in half-stepping mode which requires a sequence of 8 steps (Figures 3.7 and 3.8):

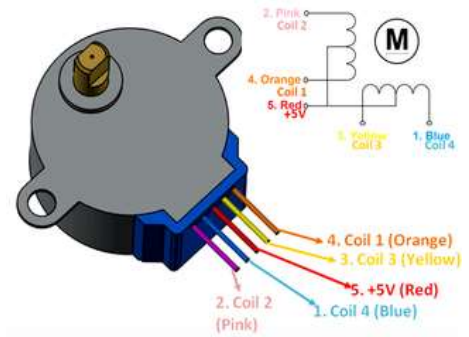


Figure 3.6: 5V Unipolar Stepper Motor

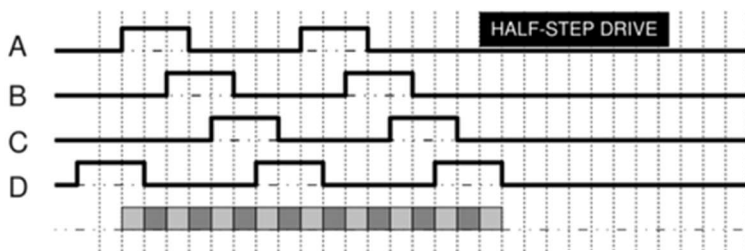


Figure 3.7: Half-Step Drive Pulse Sequence

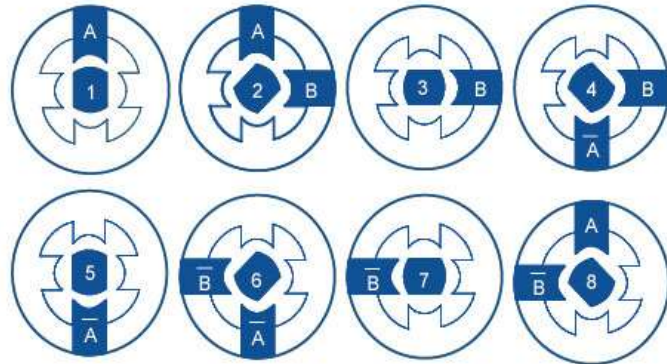


Figure 3.8: Half-Step Drive Coil Excitation

The minimum time between a step sequence (to allow the coils to de-energize) is 2ms. The speed of the stepper motor can be controlled by increasing the time between steps. When the error between the desired position of the wind turbine and its actual position is large the motor will move quickly towards the desired position. As the wind turbine approaches the desired position the error is decreased and the speed of the stepper motor decreases. The stepper motor is controlled using a PD controller.

Boost Converter

To achieve a voltage between 10V and 15V the rectified voltage produced from the generator must be boosted up to maintain the output voltage in the specified operating range. The controller is used to control the switching MOSFET in the boost converter (Figure 3.9), by changing the duty

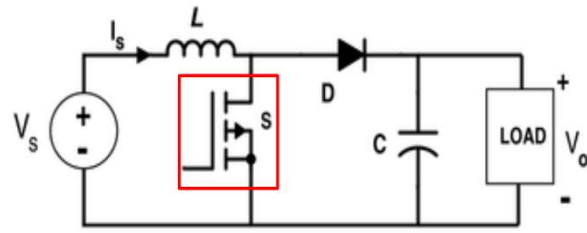


Figure 3.9: Boost Converter Circuit with Switching MOSFET

cycle of the PWM signal applied to the gate of the MOSFET. Due to the design of the generator the voltage it produces with no load is already 12V and allowing the "boosting" of the boost converter to be minimum thus increasing overall efficiency of the design.

LCD

An LCD-TFT was used to display information to the user (Figure 3.11). The display also included a touch screen layer and an I^2C touch controller to map touch inputs. The touch screen could be used to manually rotate the wind turbine clockwise or counter-clockwise, as well as, apply an electrical brake to keep the rotor from spinning as an added safety feature.

Data was written to the display using a BSP (board support package) library provided by STM. Given more time for this project a RTOS such as FreeRTOS would have been implemented instead, allowing the use of more advance graphics libraries such as TouchGFX or Embedded Wizard.

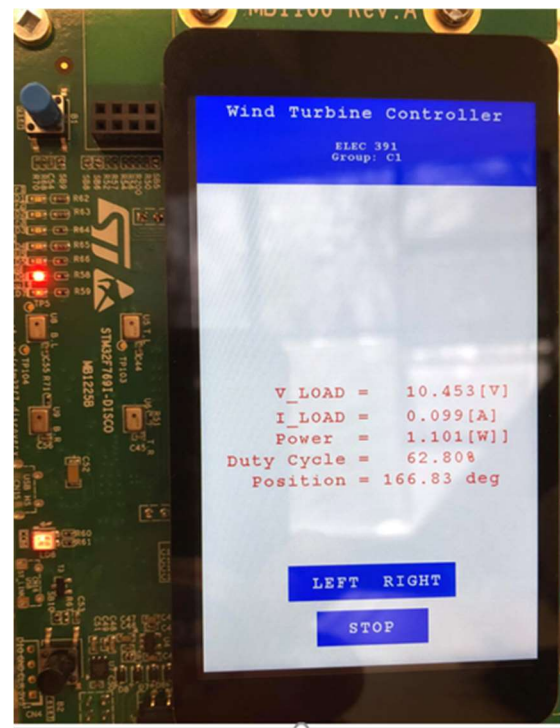


Figure 3.10: LCD Panel Displaying Readings

Maximum Power Point Tracking

When operating the specified voltage range maximum power point tracking (MPPT) is used to deliver the maximum possible generated power to the load. MPPT was implemented using a perturb and observe algorithm where the duty cycle is changed every two seconds by 2.5%. When the controller is below the minimum voltage or above the maximum voltage a proportional controller is used to bring the voltage back into the operating range. Below is a flow chart of the implemented algorithm (Figure 3.10):

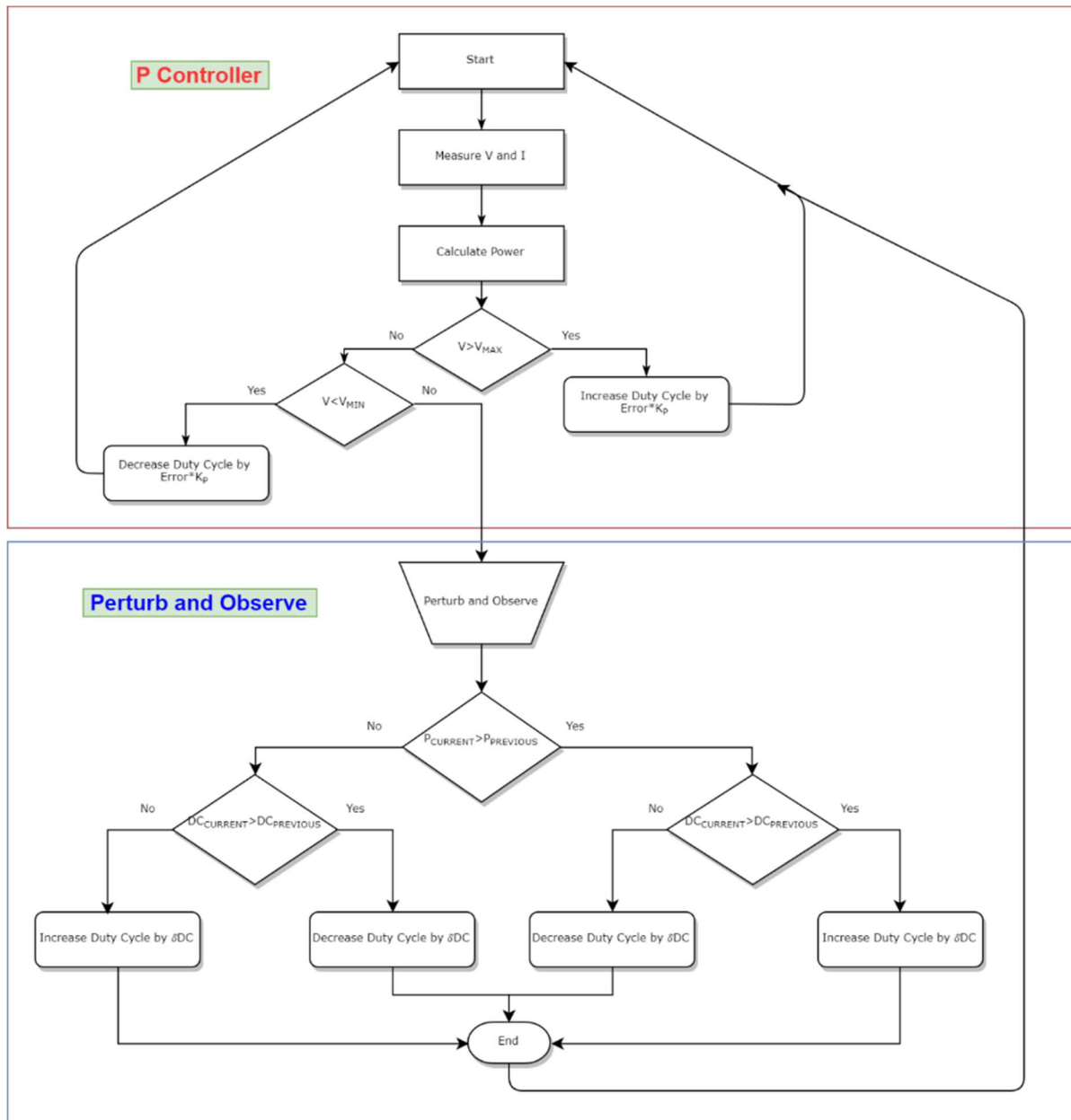


Figure 3.11: Boost Converter Control Algorithm

Validation

ADC

Comparing the calculated load voltages and currents to the ones measured using a multimeter, the readings were found to be relatively close and accurate allowing for a correct power calculation to be used with the MPPT algorithm.

Stepper Motor

Code was written to implement a PD controller but after testing the tuned parameters on the actual system it was determined that the K_d term was not necessary and was set to zero, therefore in the final implementation only a proportional controller was necessary. The K_d was set to zero because even when the stepper motor was travelling at its fastest speed, overshoot was not an issue due to relatively slow speed of the stepper motor.

LCD

The LCD was the only peripheral whose control loop was not triggered by an interrupt. Instead the updating of the LCD screen and touch input was controlled by the main application thread. This was chosen because the displaying of data to the user was deemed not to be a time critical task in comparison to the overall operation of the wind turbine. The LCD and touch input were still extremely responsive and the execution of interrupts in the background did not affect their functionality.

Maximum Power Point Tracking

Different percentages to change the duty cycle were tested and it was found that a change in 2.5% produce the best results and achieved MPPT in shortest time. A change of duty cycle of 1% would also eventually lead to MPPT but the rise time was determined to be too slow.

Task 4: Sensing and Modeling

This section covers the creation of the sensors and Simulink models used to design and tune the system. This task's main components are as follows:

- Creation and tuning of a working voltmeter circuit
- Creation and tuning of an ammeter circuit
- Design and implementation of a wind direction sensor
- Creation of a Simulink model to tune a controller for a stepper motor
- Creation of a Simulink model to tune a controller for the output voltage of the boost converter
- Determining, either through calculation or experimentation, the parameters necessary for proper response of a constant interval perturb and observe maximum power point tracking algorithm

Voltmeter

Requirements and Goals

- To receive up to 20V and map these voltages to 3.3V of an ADC channel for the microcontroller to read
- To keep power losses below 10mW
- To retain a low output impedance to allow the microcontroller to read faster as the ADC's capacitor would be able to charge faster
- To implement safeguards against negative or higher voltages than expected

Design

The final design can be seen in Figure 4.1, and the justifications for all the individual components are as follows.

To be able to read 20V as 3.3V requires a decrease in voltage by 6.06. This requirement is easily met by a voltage divider with a ratio of 5:1.

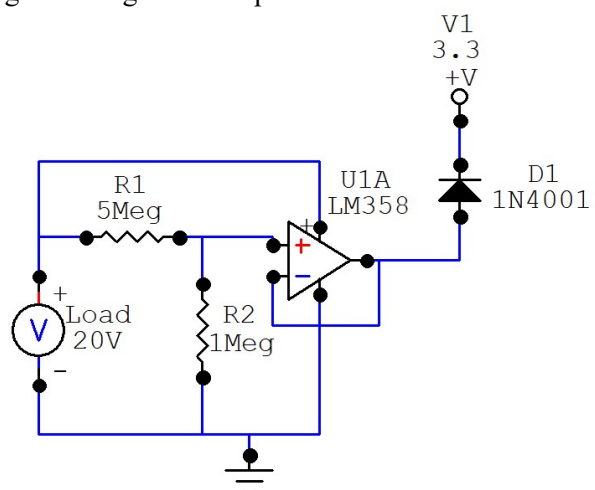


Figure 4.1: Voltmeter Circuit

Resistors of $5\text{M}\Omega$ and $1\text{M}\Omega$ were chosen as their combined resistance of $6\text{M}\Omega$ keeps the maximum power losses to $66.7\mu\text{W}$, fully meeting the power requirements.

The voltage divider precedes a voltage following operational amplifier, which fulfills the requirement of having a low output impedance. The LM358AN operational amplifier is used for 3 reasons. Firstly, this amplifier does not require a negative voltage source, allowing it to be easily connected to the ground rail of the system and is also used as protection against negative voltages. Secondly, to be able to output voltages up to 3.3V , this Op Amp needs to be able to be powered by the voltage coming out of the boost converter, which can reach up to 20V . The LM358AN can receive up to 32V as a supply voltage [16], fulfilling this requirement. Lastly, the LM358AN has 2 amplifiers on the same chip for other components, allowing for less space to be used on the final PCB and therefore reducing costs.

As a protection against voltages higher than 3.3V , a diode is put at the output of the amplifier to ensure that the output voltage cannot exceed this voltage. Due to their low voltage drop, a 1N5819 Schottky diode is placed there. To create the 3.3V , a channel from the microcontroller is connected to a second voltage following amplifier as another protection for the microcontroller. This diode is chosen for its small forward voltage drop, similarly to the boost converter.

Validation

To verify that the circuit works as intended, results from simulation and testing work are used. A plot from CircuitMaker looking at multiple voltages shows a linear output in the region being operated as shown in Figure 4.2. Tests are also done to see how close the gain was to six different voltage readings, the plot of which is noted in Figure 4.3. A line of best fit is drawn and, when using these values, the maximum error from the data was found to be limited to 1.12% .

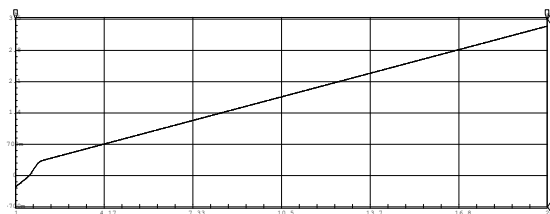


Figure 4.2: Voltmeter CircuitMaker Plot

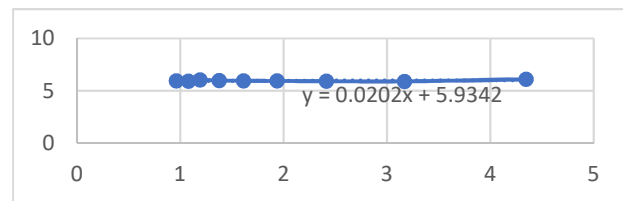


Figure 4.3: Plot of Voltmeter Gain vs Voltage Signal to Microcontroller

Ammeter

Requirements and Goals

- Receive up to 700mA and map these voltages to 3.3V of an ADC channel for the microcontroller
- To retain a low output impedance to allow the microcontroller to read faster as the ADC's capacitor would be able to charge faster
- To keep power losses below 0.25%
- To implement safeguards against negative or higher voltages than expected

Design

The final design can be seen in Figure 4.4, and the justifications for all the individual components are as follows.

To read the current through the load, a shunt resistor is placed in series with it so that the voltage can be read over it. After knowing that a 100Ω load would be used, it is determined that a 0.22Ω shunt resistor at the same current would absorb 0.22% of the power.

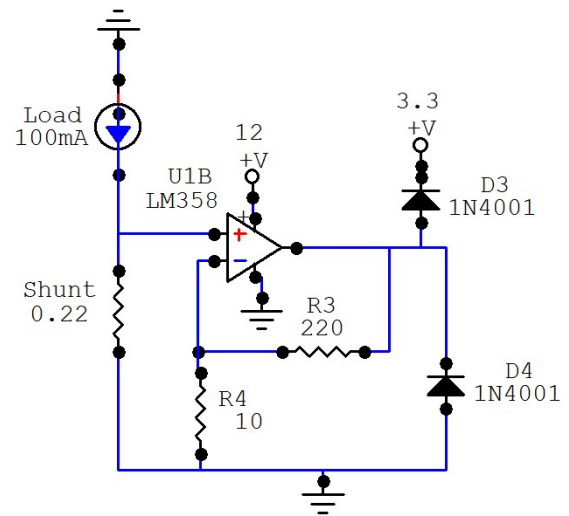


Figure 4.4: Ammeter Circuit

To be able to read 700mA as 3.3V requires an increase in voltage by a factor of 21.4. This requirement is easily met by a voltage non-inverting amplifier with a gain of 22. Resistors of 10Ω and 220Ω are chosen as their combined resistance of 230Ω ensures that the output impedance is low and the ADC can read values faster.

Another LM358AN Operational Amplifier is used for the same reasons as its use in the voltmeter.

As a protection against voltages higher than 3.3V, a diode is put at the output of the amplifier, like the voltmeter circuit. However, another 1N5819 Schottky diode is also used between ground and the output in the case that the load is opened, and the amplifier could amplify a very small, but potentially dangerous negative voltage.

Validation

To verify that the circuit worked as intended, results from simulation and testing work are used. A plot from CircuitMaker looking at multiple currents shows a linear output in the region being operated as shown in Figure 4.5. Tests are also done to see how close the gain was to 0.21 at different voltage readings, the plot of which is noted in Figure 4.3. A line of best fit is drawn and, when using these values, the maximum error found from the data was found to be limited to 0.4%.

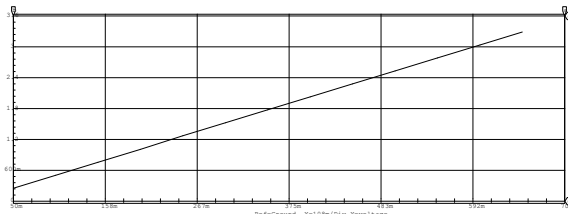


Figure 4.5: Ammeter CircuitMaker Plot

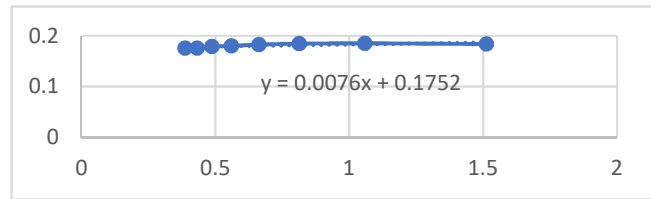


Figure 4.6: Plot of Ammeter Gain vs Voltage Signal to Microcontroller

Wind Direction Sensor

Requirements and Goals

- To turn behind the spinning blades of the wind turbine
- Read 300 degrees mapped on a 3.3V ADC of the microcontroller

Design

To know the absolute location of the wind direction rather than the relative position, a wind vane is mounted onto a linear rotary potentiometer capable of rotating 300 degrees, fed by 3.3V from the microcontroller and read directly by one of the ADC channel pins.

To improve the rotation of the potentiometer, two major mechanical aspects are implemented in the final product. The first is that the rotary potentiometer is opened and the grease on the inside is removed using WD40, allowing for more free movement. Secondly, a tail is added with a wider back portion, as seen in Figure 4.7 to allow the wind direction sensor to have a steadier final location, as there will be more air friction on either side.

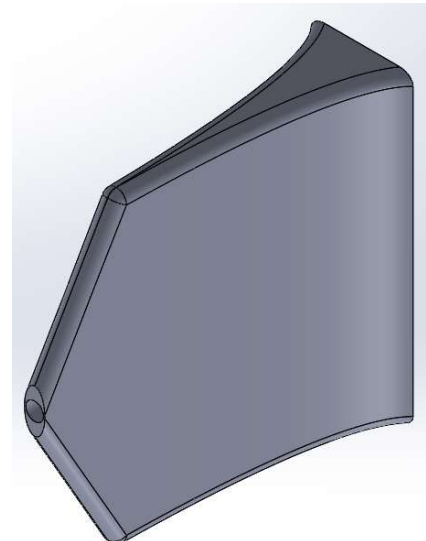


Figure 4.7: Fin on Wind Vane

Validation

Based upon the accuracy of the ADC, the error of any given reading between 0 to 4095 being mapped between 0 and 300 degrees gives an error of $300/4095 = 0.07$ degrees. Another large component of error is the fact that the air reaching the sensor is non-linear, resulting in a constant 17-degree error to one side, compensated for by the microcontroller.

Stepper Motor Controller

Design

The stepper motor Simulink model is designed to represent the control loop for accurate position

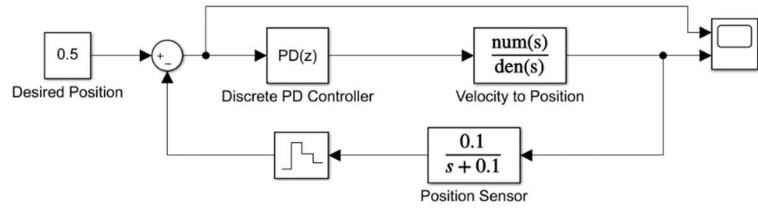


Figure 4.8: Stepper Motor Control Loop

control and is depicted in Figure 4.8. It has the following major components:

- Transfer function mapping velocity of the motor to the position of the turbine
- Transfer function modelling the position sensor as a time delay
- A discrete PD controller to adjust the speed of the stepper motor

The velocity of the stepper motor mapped to the position of the wind turbine has four major components, seen in the equation $T(s) = \frac{360}{6.4 \cdot 512 \cdot s} * 360$ represents the amount of degrees of rotation, 512 is the number of steps of the stepper motor, 6.4 is the gear ratio, and the s in the denominator is for conversion from velocity into speed, as it is the integral.

The position sensor is represented with a low pass filter, seen in the equation $P(s) = \frac{0.1}{s+0.1}$. This assumes a worst-case scenario where the 1% settling time is 10 seconds, which only happens during the initial operation of the fan.

A PD controller is chosen because the integral component is unnecessary, given that a fast response is desired and the integral component would take too long to take effect. The D component is originally desired to eliminate overshoot. The PD controller contains two major parts and is designed around operating every 100ms, which is the fastest speed the microcontroller can sample and average, given the output

impedance of the potentiometer. The P component is designed around having a desired scenario where having the position sensor reading a 45-degree error will result in the maximum speed of the motor being used, which is 500 Hz. This is to ensure that the position sensor does not stray too far, and if it does the stepper motor operate at its fastest speed. This results in a K_P value of $500/45 = 11.111$. The K_D value, using Simulink's PID Tuner App, is found to be 100.

Validation

The output of the simulation is shown in Figure 4.9, which shows a fast but not overshoot response to the desired position.

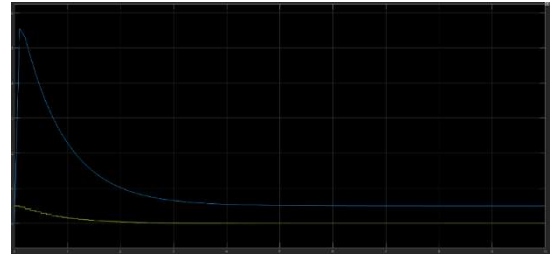


Figure 4.9: Stepper Motor Simulation Output

Output Voltage Controller

Design

A closed-loop Simulink model is used to accurately design a controller for the output voltage of the boost converter, whose Simulink model is depicted in Figure 4.10. it is made up of the following major components:

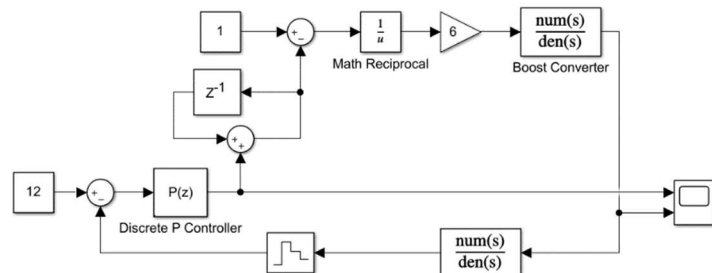


Figure 4.10: Output Voltage Control Loop

- Model mapping duty cycle to output voltage
- Transfer function modelling the time delay of the boost converter
- Transfer function modelling the time delay of the voltage sensor
- A discrete P Controller to adjust the duty cycle of the boost converter

The duty cycle mapped to the output voltage is done using the equation $V_o = \frac{V_i}{1-D}$. This is assuming that the input voltage remains constant, which is only an acceptable approximation when decreasing the output voltage. This is because the output voltage will decrease faster than the input voltage will increase, whereas the opposite is true when trying to increase the output voltage.

The boost converter is represented with a low pass filter, seen in the equation $B(s) = \frac{188000000}{s+188000000}$. This is found using the bode plot from the Multisim model of the boost converter, shown in Figure 4.11.

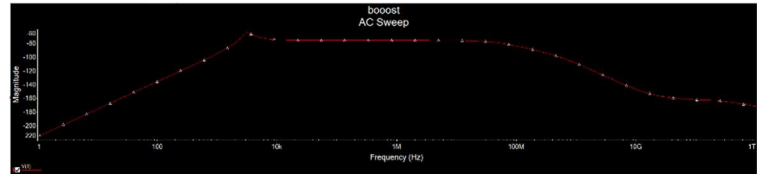


Figure 4.11: Boost Converter Bode Plot

The voltage sensor is represented with a low pass filter, seen in the equation $V(s) = \frac{15400}{s+15400}$. This is found using the bode plot from the CircuitMaker model of the voltage sensor, shown in Figure 4.12.

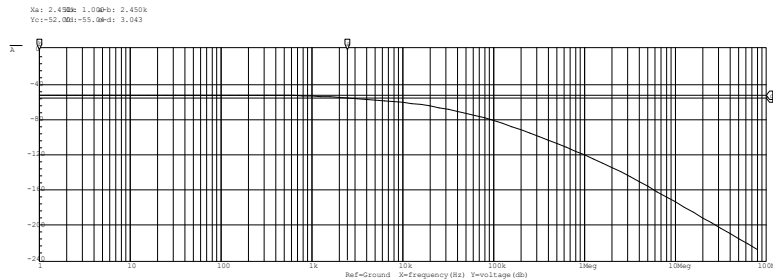


Figure 4.12: Voltmeter Bode Plot

A P controller is chosen for its ability to quickly and easily drop the output voltage whenever necessary, which will only ever be the case when it exceeds 15 volts. Using the PID Tuner App in Simulink, the value for P is found to be $K_p = 1$.

Validation

The output of the simulation is shown in Figure 4.13, which shows a fast response to decreasing the output voltage to the desired position.

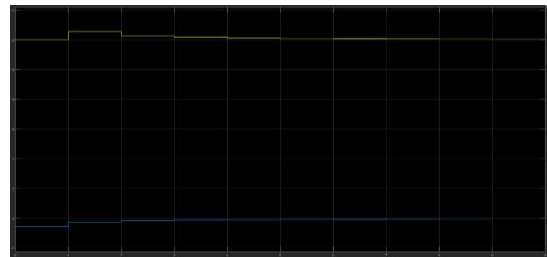


Figure 4.13: Output Voltage Simulation Output

Perturb and Observe Algorithm

Design

A constant interval perturb and observe MPPT algorithm is used and has two aspects to its design:

- Time between perturbances
- Quantity of perturbances

There are two major time delays to be considered. The first is the time delay of the change of the physical system, which is experimentally found to be approximately 1.66 seconds. Next is the settling time of the boost converter, found to be:

$$t = 2 \cdot \pi \cdot \sqrt{L \cdot C} \cdot 20 = 2 \cdot \pi \cdot \sqrt{1.012m \cdot 220u} \cdot 20 = 59.3ms$$

Due to this added time and other possibly unseen factors that affect the settling time, the time between perturbances is increased to 2 seconds.

The amount that the duty cycle is changed by is 2.5%, experimentally determined to be the amount needed to escape local maxima in the power curve and reach the absolute maximum.

Integration Process

Power Electronics with Generator

For the first stage of the integration process, the generator was first tested with the 3-phase rectifier and then with the boost converter as well. Tests with the rectifier included changing the load and measuring the voltage and current at the load to calculate the power. The calculated powers were then plotted against the resistance values to provide a basic power curve, shown in Figure 5.1 below, from which our maximum power could be determined. While testing, we observed that any loads below $65\ \Omega$ prevented the blades from overcoming initial cogging torque and reaching maximum speed. To solve this, we used a switch to change the resistance once the blades reached to speed with a higher load.

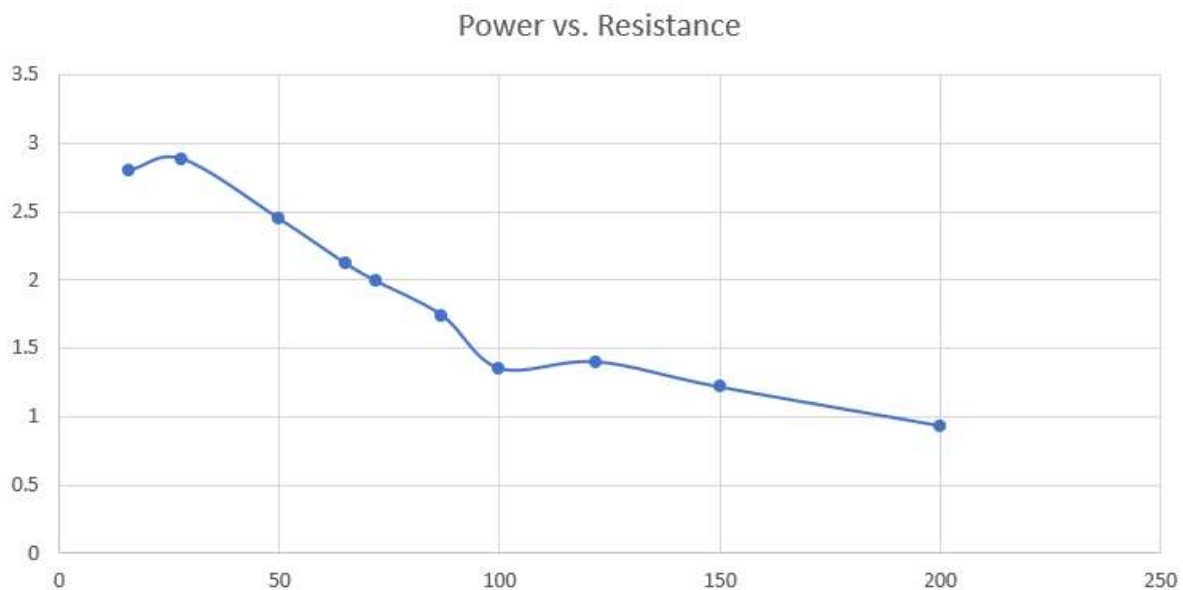


Figure 5.1: Power vs Resistance Curve

The next part included testing different duty cycles with the boost converter to determine if everything was functioning as it should and to give us a better and more accurate idea of the power we were generating. While testing we found that although we measured higher powers with lower loads, our maximum voltage decreased as well. Resistances less than $65\ \Omega$ prevented us from achieving voltages higher than 10 V and so a $100\ \Omega$ load, which resulted in an average voltage of approximately 12 volts at max power, was used.

Sensors with Power Electronics and Controller

During this stage of the integration process, the voltage and current sensors are added on to the existing PCB for the power electronics, seen in Figure 2.6, where the final calibration of these values reduces the respective errors to 1.12% and 0.4%. The outputs of these sensors are connected directly to the channels of the microcontroller for fast and readily-available data transfer.

The position sensor is mounted above the main generator, close to the edge of the turbine blades, where there is higher wind speed for the wind vane to turn with. After wiring the potentiometer directly to the microcontroller, the non-linear air coming out of fans is discovered to be a consistent 17 degrees.

Stepper Motor Control and Maximum Power Point Tracking Testing

During this stage, both control loops are tested to determine their ability to have the desired outputs. For the stepper motor control loop, it is determined that the K_d component of the control loop has little to no visible effect on the ability of the turbine to turn towards the fan. This is due to the slow maximum speed of the motor resulting in very little to no overshoot and very accurate precision of steps. For the MPPT algorithm, it is noticed that any perturbation lower than 2.5% results in occasionally getting stuck in local minima and not outputting maximum power.

Battery Charging and Powering Connections

During this stage of integration, the 12V lead acid battery charger circuit was constructed and attached to the final wind turbine structure. The circuit is built around the UC3906 battery charger IC, following the schematic included on the datasheet [12]. The battery used is a 12V 1.3Ah lead acid battery which, when connected, can power the microcontroller and all the peripherals [13]. Once the turbine is spinning at max power, the battery charging circuit begins the charging process. The purpose of the battery and charger circuit is to allow for the wind turbine to become self-sufficient while also being able to maintain power during low or no wind situations. A 1N5819 diode was placed between the boost converter and the battery charger circuit to the voltage of the battery to interfere with the voltage which the converter is creating. The following figure visually demonstrates how the boost converter, battery charger and the microcontroller were connected for the final implementation.

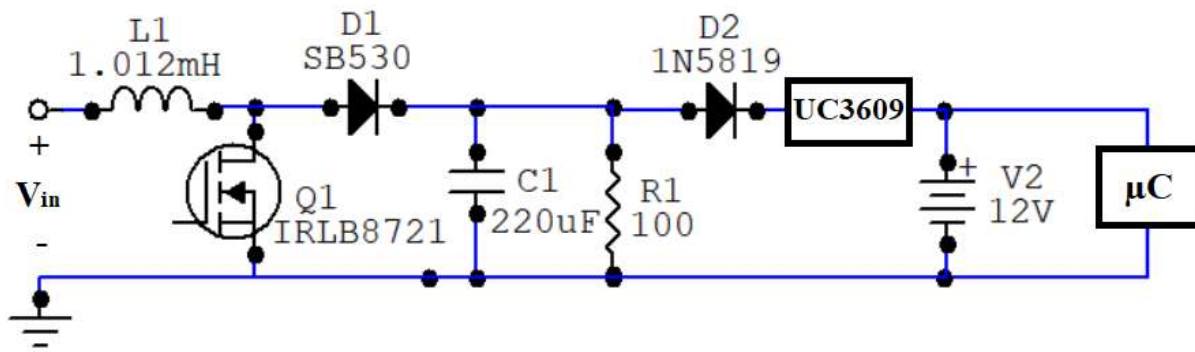


Figure 5.2: Battery Charging Circuit Connection Diagram

Final Construction and Testing with Fans

The final assembly of the wind turbine, with Meccano parts making up build the main tower, is tested for proper performance and operation. The MPPT algorithm settles to around 40% and at maximum speed settings, produces 2.033 Watts at 14.3 Volts. This power is used to charge the lead-acid battery which in turn powers the microcontroller and will also turn up to 360 degrees to face the proper direction. This was done using less than \$250 for the creation of the final prototype.



Figure 5.3: Final Product

References

- [1] İ. Tarımer, C. Ocak, “Performance Comparison of internal and External Rotor Structured Wind Generators Mounted from Same Permanent Magnets on Same Geometry,” *Elektronika Ir Elektrotehnika*, vol. 92, no. 4, Jan., pp 65- 70, 2009.
- [2] Radial Magnets Inc. “8110 Radial Magnet,” Radial Magnet datasheet, N.D.
- [3] Vishay, “Schottky Barrier Plastic Rectifiers – 1N5817, 1N5818, 1N5819,” 1N5819 datasheet, July. 2006. [Revised Aug. 2013].
- [4] Vishay, “Schottky Barrier Rectifiers SB520 thru SB560,” SB530 datasheet, Oct. 2009. [Revised Feb. 2017].
- [5] Power Electronics, *Power Electronics – Boost Converter*. 2018 [Online]. Available: https://youtu.be/AMESgY_pdMw. [Accessed: 15- Jan- 2019].
- [6] International Rectifier, “IRFZ44nPbF HEXFET Power MOSFET,” IRFZ44N datasheet, Mar. 2001. [Revised Sep. 2010].
- [7] Bourns, “5200 Series – Hash Choke,” 1mH Cylindrical Inductor datasheet, Jan. 2003 [Revised Jun. 2011].
- [8] Riedon, “Aluminum Housed Power Wirewound Resistors,” 100 Ω Power Resistor datasheet, Dec. 2012.
- [9] Bourns, “Low Core Loss, High Current Toroid Inductors,” 1mH Toroidal Inductor datasheet, Jun. 2007.
- [10] International Rectifier, “IRLB8721PbF HEXFET Power MOSFET,” IRLB8721 datasheet, Apr. 2009.
- [11] Tyco Electronics, “BUCHANAN Terminal Blocks,” Terminal Block 2.54mm pitch datasheet, Jun. 2007.

- [12] Texas Instruments, “Sealed Lead-Acid Battery Charger,” UC3906 datasheet, Sept. 1996 [Revised May. 2005].
- [13] EverExceed, “Sealed Rechargeable Lead Acid Battery,” 12V 1.3Ah Lead Acid Battery datasheet, Oct. 2008.
- [14] ST, “How To Get the Best ADC Accuracy In STM32 Microcontrollers,” STM32 ADC datasheet, Feb. 2017.
- [15] ST, “STM32F76xxx and STM32F77xxx Advanced ARM-based 32-bit MCUs,” STM32F69NI manual, Mar. 2018.
- [16] ST, “ARM Cortex-M7 32b MCU+FPU, 462DMIPS, up to 2MB Flash/512+16+4KB RAM, USB OTG HS/FS, 28com IF, LCD, DSI,” STM32F769NI datasheet, Sept. 2017.
- [17] Fairchild Semiconductor Corporation, “LM2904,LM358/LM358A,LM258/LM258A,” LM358AN datasheet, Aug. 2002 [Revisited Mar. 2019].

Appendix

Timeline:



Budget:

This is the total quantity of budget spent on the final prototype and all its individual components, broken down by task.

<u>Sensing and Modelling</u>			
Ammeter			
#	Part No.	Description	Price(\$)
1	LM358AN	Op Amp	1.33
11		Standard Resistors	0.37
2		220 m Ω Resistor	1.12
2		Schottkey Diodes	1.54
Wind Direction Sensor			
#			
1		Rotary Potentiometer	0
Voltmeter			
#			
2	LM358AN	Op Amp	1.33
6		Resistors	0
1		Schottkey Diode	0.77
<u>Generator</u>			
#	Part No.	Description	Price(\$)
16	469-1039-ND	Neodinium Magnets	20.44
2		Ball Bearings	0
1		Waterjet Cut Order	65
<u>Controller</u>			
#	Part No.	Description	Price(\$)
1		STM32F769 discovery kit	0
1		Proto-Screwshield Wingshield R3	22.25
<u>Power Electronics</u>			
Diode Rectifier			
#	Part No.	Description	Price (\$)
6	SB530	Schottky Diode	4.62
1		120 μ F electrolytic capacitor	0
1		100 Ω 10W Resistor (load)	0

Boost Converter			
#	Part No.	Description	Price(\$)
2		3 Pin Terminal Block	0
1	SB530	Schottky Diode	3.48
1		220 μ F Electrolytic Capacitor	0
1		1.5 nF Foil Capacitor	0
5		2 Pin Terminal Block	0
1		PCB	60.99
1		1.012mH Toroid Inductor	7.55
<u>Integration/Additional Features</u>			
#	Part No.	Description	Price(\$)
1		Perfboard	4.24
1		Battery Charging IC - UC3906	11.83
5		Resistors	0
1		Battery	0
Total			206.86